Coastal Marine Science 31(1): 30–39, 2007

A numerical experiment on ocean circulations forced by seasonal winds in Suruga Bay

Kiyoshi TANAKA[1]*, Yutaka MICHIDA[2] and Teruhisa KOMATSU[3]

[1] *Center for Advanced Marine Research, Ocean Research Institute, The University of Tokyo*
**E-mail: ktanaka@ori.u-tokyo.ac.jp*
[2] *Center for International Cooperation, Ocean Research Institute, The University of Tokyo*
[3] *Department of Marine Bioscience, Ocean Research Institute, The University of Tokyo*

Received 8 June 2006; Accepted 15 September 2006

Abstract—We investigate influence of the seasonal variation in the wind field on water circulation in Suruga Bay by using a wind data set and a numerical ocean model. Counterclockwise vorticity is supplied around the bay mouth from the atmosphere into the ocean in January (winter) and April (spring), whereas clockwise vorticity is supplied in July (summer) and October (autumn). Corresponding to the change in the wind field, a counterclockwise circulation is generated at the sea surface around the bay mouth in January and April, whereas a clockwise circulation in July and October. Moreover, one or two weak circulations are generated to the north of the circulation. These circulations, which are quasi-geostrophic and strongly influenced by land and ocean bottom topography, are generated without effect of the Kuroshio current. Quasi-stagnant and convergent regions tend to appear in the surface layer in the eastern part of the bay, except for autumn. There is a possibility that the wind-driven circulations may play an important role in transport of floating materials, such as seagrass, from in and around the bay to the eastern part of the bay, where a large amount of seagrass has been observed both on the sea surface and floor.

Key words: Suruga Bay, ocean circulation, seasonal winds, numerical experiment

Introduction

Suruga Bay is located south of Shizuoka Prefecture, where the wind field is strongly influenced by the land topography, such as Mount Fuji. On the other hand, the southern boundary of Suruga Bay, where the maximum water depth is greater than 2000 m, is open to the North Pacific Ocean. Therefore, water circulations in the bay are complicated in general, being strongly influenced by atmospheric variation over the bay and oceanic variation outside of the bay.

One of the factors controlling long-term circulations in the bay is the Kuroshio current, which flows along the southern coast of Japan. (In this study, we use the terminology "long-term" to refer to a duration over a diurnal tidal cycle.) Inaba (1982, 1984) showed that a counterclockwise (cyclonic) circulation tends to appear at the mouth of the bay, when the Kuroshio current flows north of the Zenisu Ridge, which is located about 80 km south of the mouth of Suruga Bay. On the other hand, a clockwise (anticyclonic) circulation tends to appear at the bay mouth, when the Kuroshio current flows south of the Zenisu Ridge. The flow speed is 0.1–0.3 m s^{-1} near the sea surface (10–20 m depth) at the eastern and western edges of the bay mouth. Recently, Katsumata (2004) has shown that variability with a period of half to one month in the flow field is strongly related to the Kuroshio current variability.

Buoyancy-driven coastal currents may also contribute to the long-term circulations in the bay. Unoki and Okami (1985) showed that river discharge from Fuji, Abe and Ooi Rivers supports the presence of a counterclockwise circulation in the bay, since the river waters turn to the right after they run into the sea. However, their analysis based on only the LANDSAT satellite images was rather qualitative.

Kyucho, which is a sporadic event associated with strong currents, plays an important role in terms of water exchange between the bay and the North Pacific. Katsumata (2004) estimated that 45–70% of the total water volume in Suruga Bay is exchanged by an event. This phenomenon is triggered by Kuroshio warm water intrusion (Katsumata, 2004) or a typhoon passing by (Igeta et al., 2003). The time scale of Kyucho is a few or several days at most.

Although influence of tides on the long-term circulations is still not clear, tidal flows in Suruga Bay have been investigated by many studies. Inaba (1981) showed that diurnal constituents dominate over semidiurnal ones in the flow field, whereas the latter dominate over the former in the sea level variation, suggesting that the tidal flow has a strong baroclinic structure. Indeed, it has been observed that tidal currents are amplified toward the bottom in the bay (Matsuyama et al., 1993), being strongly affected by the steep bottom topography (Takeuchi and Hibiya, 1997).

The wind also plays an important role in driving flow in the bay, especially in a shallow layer. Katsumata (2004) showed a significant coherence between fluctuations of atmospheric wind and oceanic flow at periods shorter than 10 days. That is, when the wind direction is easterly (westerly), near-surface water flows into (out of) the bay at the eastern part of the bay mouth, suggesting the presence of a counterclockwise (clockwise) circulation around the bay mouth. On the other hand, influence of the atmospheric variation on the long-term circulations with a time scale longer than 10 days has hardly been investigated. However, since Suruga Bay is large enough for geostrophic currents to be generated (i.e., small Rossby number; for example, $R_o(=U/fL)\approx 0.18$, where $U=3.0\times10^{-1}\,\mathrm{m\,s^{-1}}$, $f=0.83\times10^{-4}\,\mathrm{s^{-1}}$ and $L=2.0\times10^{4}\,\mathrm{m}$), significant geostrophic circulations may be generated in the bay, if the wind stress provides a sufficient source of vorticity in the ocean.

As well known, the wind field over Suruga Bay varies temporally and spatially. In particular, it is expected that in a coastal region such as Suruga Bay, seasonal variation of the wind field will play an important role in generating variation in the long-term circulations. In this study, therefore, we investigate the influence of the seasonal variation in the wind fleld on the water circulations in Suruga Bay by using a numerical model.

Materials and Methods

Seasonal variation in the wind field

Before carrying out the numerical integration, we investigate the seasonal variation in the wind field over and around Suruga Bay, by using a meso-regional objective analysis (MANAL) data of the Japan Meteorological Agency (JMA). The three-dimensional gridded data of wind velocity with a horizontal resolution of about 10 km has been produced on the basis of ground, upper-air and satellite observational data.

Figure 1 shows monthly mean fields of sea surface wind stress forcing over and around Suruga Bay for January, April, July and October 2003. The wind speed data is converted to wind stress data, by using the formula given by Large and Pond (1981) and Kutsuwada (1998). The wind (stress) varies considerably in time and space. There are strong westerly winds in January, whereas easterly in October. Moreover, it should be noted that in these months, the wind stress is reduced inside of the bay, whereas it is strong outside of the bay. This means that significant wind stress curl is generated over the bay mouth ($curl\ \tau=\partial\tau_y/\partial_x-\partial\tau_x/\partial_y$, where τ_x and τ_y are longitudinal and latitudinal components of the wind stress, respectively, and x and y are longitudinal and latitudinal coordinates, respectively). In other words, significant positive (counterclockwise) vorticity is supplied around the bay mouth from the atmosphere into the ocean in January, whereas negative (clockwise) vorticity is supplied in October.

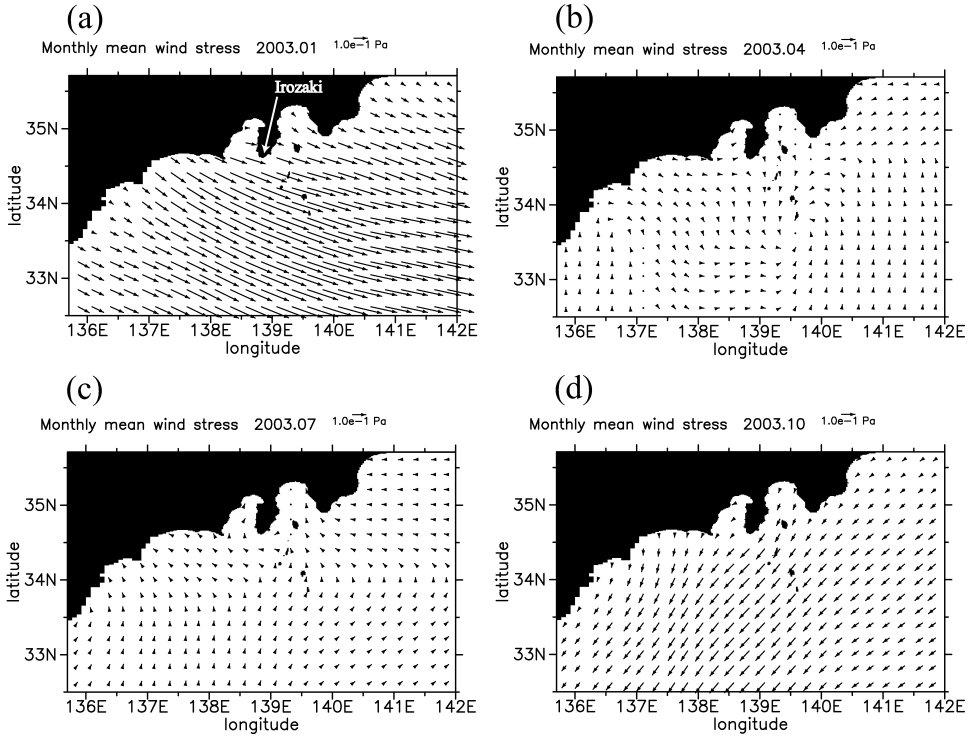

Fig. 1. Distributions of monthly mean wind stress in and around Suruga Bay: (a) January 2003, (b) April 2003, (c) July 2003, and (d) October, 2003. An arrow in (a) indicates the location of Irozaki.

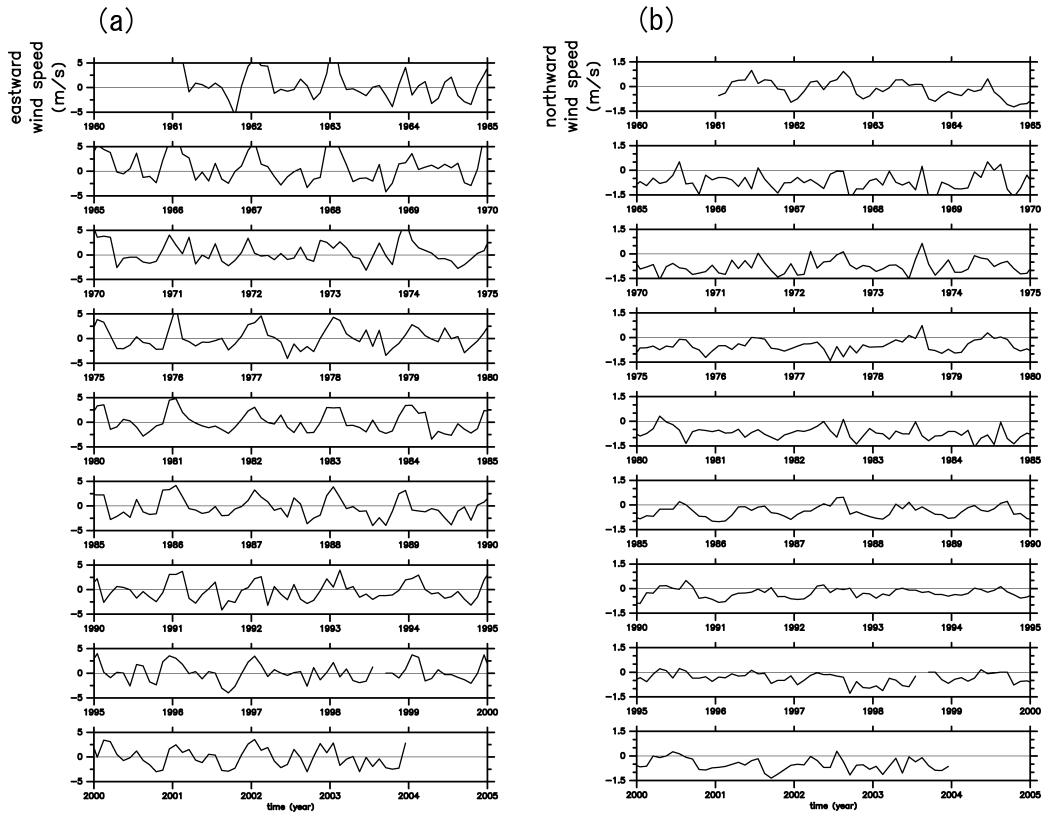

Fig. 2. Time changes of monthly mean wind speeds which have been observed at the Irozaki meteorological station (the location is indicated by an arrow in Figure 1(a)): (a) eastward speed and (b) northward Speed.

On the other hand, there are only weak winds in April and July. However, the weak westerly winds rotate counterclockwise in the bay in April, whereas the weak easterly winds rotate clockwise in July. Thus, significant positive (counterclockwise) vorticity is supplied around the bay mouth from the atmosphere into the ocean in April, whereas negative (clockwise) vorticity is supplied in July, although the wind stress is not so strong as in January and October.

Figure 2 shows time changes of one-month running mean values of wind speed (westerly and southerly components), which have been observed at the Irozaki weather station by JMA (the location is indicated by a white arrow in Figure 1a). The strong westerly and easterly winds tend to be observed every winter and autumn, respectively. On the other hand, weak westerly and easterly winds tend to be observed every spring and summer, respectively. Thus, it is suggested that the wind fields shown in Figure1 represent climatological seasonal variation of the wind fields. It is also suggested that the vorticity supply mentioned above varies seasonally: that is, significant positive (counterclockwise) vorticity is supplied around the bay mouth from the atmosphere into the ocean in winter and spring, whereas negative (clockwise) vorticity is supplied in summer and autumn.

Numerical model configuration

The ocean model is based on the GFDL Modular Ocean Model (MOM) 2.2β (Pacanowski, 1996). The model domain extends from 135.7°E to 142.0°E and 32.5°N to 35.71°N, and the maximum depth is 1100 m (Figure 3). The longitudinal grid spacing is 0.0125° in and around Suruga Bay (the region enclosed by dashed lines in Figure 3a), and it increases smoothly to 0.075° and 0.0375° at the artificial western and eastern boundaries of the model basin, respectively. The latitudinal spacing is 0.01° in and around the bay, increasing smoothly to 0.04° at the artificial southern boundary. There are 14 levels in the vertical, with a spacing of 5 m at the surface, smoothly increasing to about 240 m on the bottom (Table 1). The bottom topography is derived from the J-EGG500 data compiled by Japan Oceanographic Data Center.

The governing equations are primitive equations in a spherical coordinate system under the Boussinesq, hydrostatic and rigid-lid approximations. The Smagorinsky scheme is adopted to calculate the horizontal turbulent momentum viscosity and turbulent tracer diffusivity coefficients with the adjustable constant of 0.28 (Smagorinsky, 1963; Rosati and Miyakoda, 1988). This value in this study, which is twice that ordinarily used, is chosen to take into consideration the strong tidal mixing in Suruga Bay. The coefficients for the vertical turbulent momentum viscosity (ν_z) and turbulent tracer diffusivity (κ_z) are given by

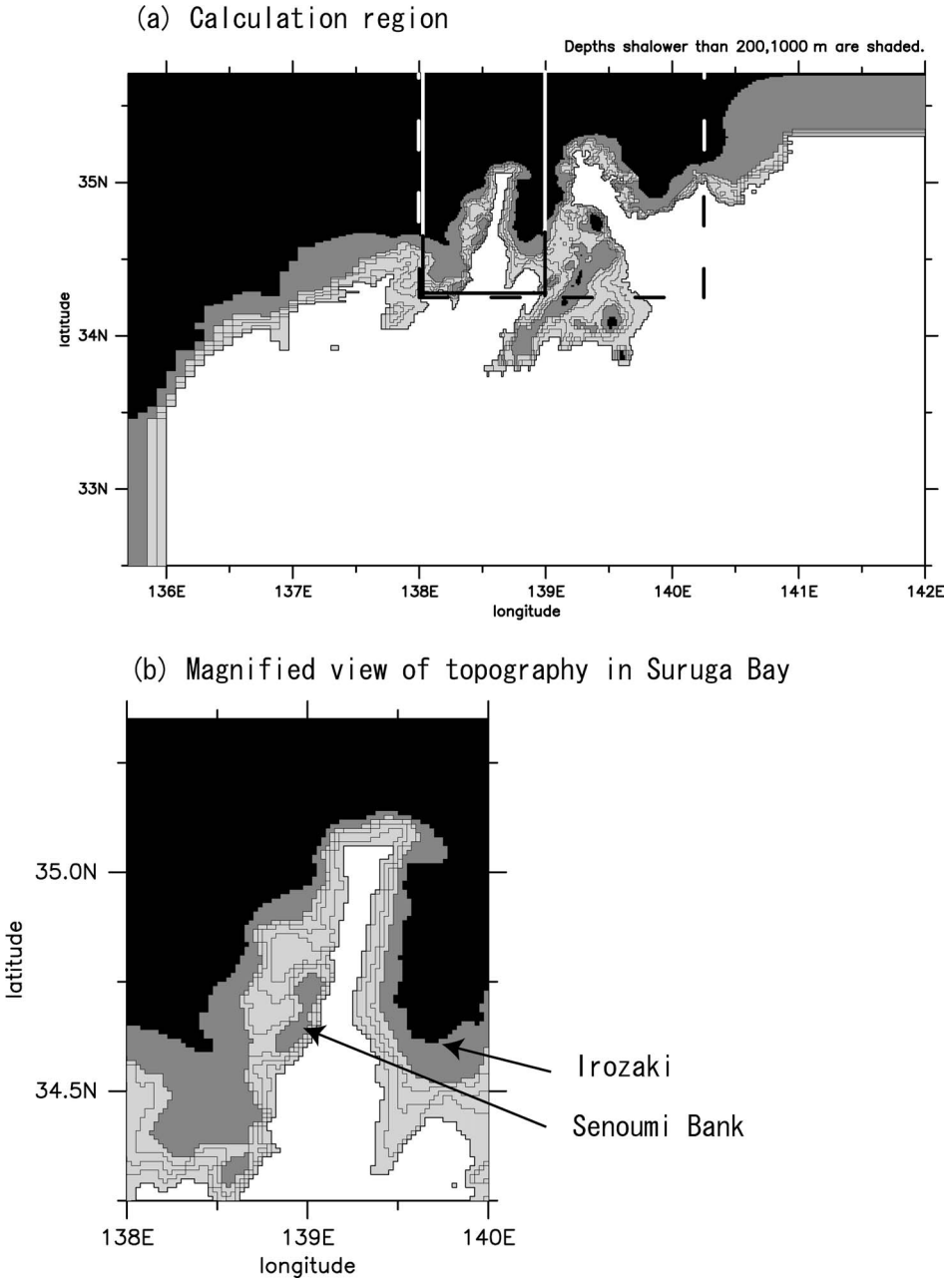

Fig. 3. Model region and topography with contour interval of 200 m. (a) Calculation region. Horizontal resolution is 0.0125°×0.01° in the region enclosed by dashed lines. (b) The region of main interest, enclosed by solid lines in (a).

$$\nu_z = \nu_r + \nu_{back}, \quad \text{for } z \geq -100\text{m},$$
$$\nu_z = \min\{\nu_r + \nu_{back}, \nu_{lim}\}, \quad \text{for } z < -100\text{m}, \tag{1}$$
$$\kappa_z = \kappa_r + \kappa_{back}, \quad \text{for } z \geq -100\text{m},$$
$$\kappa_z = \min\{\kappa_r + \kappa_{back}, \kappa_{lim}\}, \quad \text{for } z < -100\text{m}, \tag{2}$$

where

$$\nu_r = \frac{\nu_0}{1.0 + Ri}, \tag{3}$$

$$\kappa_r = \frac{\kappa_0}{(1.0 + Ri)^2}, \tag{4}$$

$$Ri = \frac{g \dfrac{\partial \rho}{\partial z}}{\rho \left(\dfrac{\partial \rho}{\partial z} \right)^2}. \tag{5}$$

In the above equations, z is the coordinate (positive upward, $z=0$ at the sea surface), g ($=9.8\,\text{m s}^{-2}$) is the acceleration of gravity and ρ is the water density. ν_r and κ_r are the vertical mixing schemes of Officer (1976), which was derived on the basis of coastal observations. In this study we set $\nu_0 = \kappa_0 = 1.0 \times 10^{-2}\,\text{m}^2\,\text{s}^{-1}$, taking into consideration near-surface mixing which is induced by strong winds around Suruga

Table 1. Depths and thickness of model levels.

Level	Depth (m)	Thickness (m)
1	2.5	5.0
2	7.5	5.0
3	12.5	5.0
4	17.5	8.8
5	30.0	16.3
6	50.0	20.0
7	70.0	24.2
8	98.4	40.3
9	150.6	70.1
10	238.5	109.0
11	368.5	151.0
12	540.6	189.9
13	748.4	219.7
14	980.0	235.8

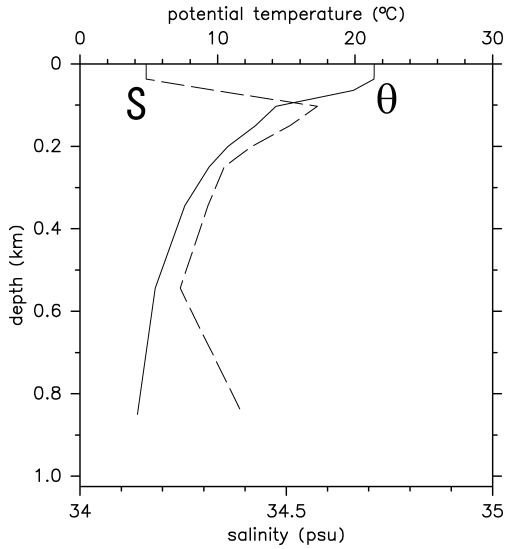

Fig. 4. Vertical profiles of potential temperature and salinity at initial.

Bay. $\nu_{back}(=1.0\times10^{-3}\,\mathrm{m^2\,s^{-1}})$ and $\kappa_{back}(=3.0\times10^{-5}\,\mathrm{m^2\,s^{-1}})$ are background values. However, the final coefficients do not exceed $\nu_{lim}(=1.5\times10^{-3}\,\mathrm{m^2\,s^{-1}})$ and $\kappa_{lim}(=4.5\times10^{-5}\,\mathrm{m^2\,s^{-1}})$ in the region deeper than 100 m.

Since our focus is on the wind-driven circulations, we consider initial conditions in which fluid is at rest and potential temperature and salinity fields are horizontally uniform, whose vertical profiles shown in Figure 4 were obtained near the center of Suruga Bay in autumn (Nakamura and Sawada, 1971). That is, low-salinity water that originates in rivers is located in the near-surface layer shallower than 50 m. On the other hand, high-salinity water with a salinity maximum of 50–200 depth originates in the Kuroshio current. Below this depth, low-salinity water with a salinity minimum is located, which originates in the intermediate water in the subpolar gyre region. A thermocline, which is important in terms of dynamic processes, is located at 50–100 m depth.

At the coastal and artificial northern and western boundaries, closed boundary conditions are applied (no-slip and no buoyancy flux conditions). At the artificial southern and eastern boundaries, on the other hand, semi-open boundary conditions are applied as follows: Baroclinic velocity components (deviation from the depth-averaged velocity) are calculated by a linearized momentum equation, according to Stevens (1990). On the other hand, the closed boundary condition is applied for the barotropic (the depth-averaged) component. Boundary values of potential temperature and salinity (buoyancy flux) are calculated on the basis of passive (radiation) conditions after Stevens (1990). Moreover, sponge layers, where the potential temperature and salinity are restored to the initial values with a restoring time scale of 5 days, are applied within about 1.0° of the artificial southern and eastern boundaries. Therefore, significant artificial upwelling/downwelling due to Ekman divergence/convergence at the boundaries do not occur. Furthermore, since the total water depth is at most 1100 m in the model, the potential temperature and salinity in the deepest grid boxes (vertical level 14) are restored to the initial values with a timescale of 30 days.

In the next section we describe results for four experimental cases (January, April, July and October), in which the circulations are driven only by the monthly mean wind stress shown in Figure 1. In the present study, as a first step to understand the effects of seasonal winds on the circulations, we assume the wind stress to be constant in time. Moreover, we apply only the vertical profiles of potential temperature and salinity in autumn (Figure 4) to all the experiments, although they vary seasonally, especially near the sea surface, in the real ocean.

Results and Discussion

Experimental results

Figure 5a shows a distribution of horizontal velocity in the sea surface layer on day 60 and Figure 5b shows a time change of kinetic energy integrated over the entire model domain in the case of January. The flow field approaches a quasi-steady state until day 60, judging form the evolution of kinetic energy. Although the domain size of the model is much larger than that of Suruga Bay, the spin-up time is shorter than the seasonal timescale. Thus, it is suggested that in the real ocean as well as in the model, the flow field will respond to the atmospheric seasonal cycle significantly. In the following analysis we investigate the flow field on day 60, especially in the region shown in Figure 3b.

Figure 6 shows distributions of horizontal velocity in the sea surface layer. A strong large-scale circulation with counterclockwise rotation is generated across the bay mouth in January (Figure 6a), when the wind stress is stronger than in

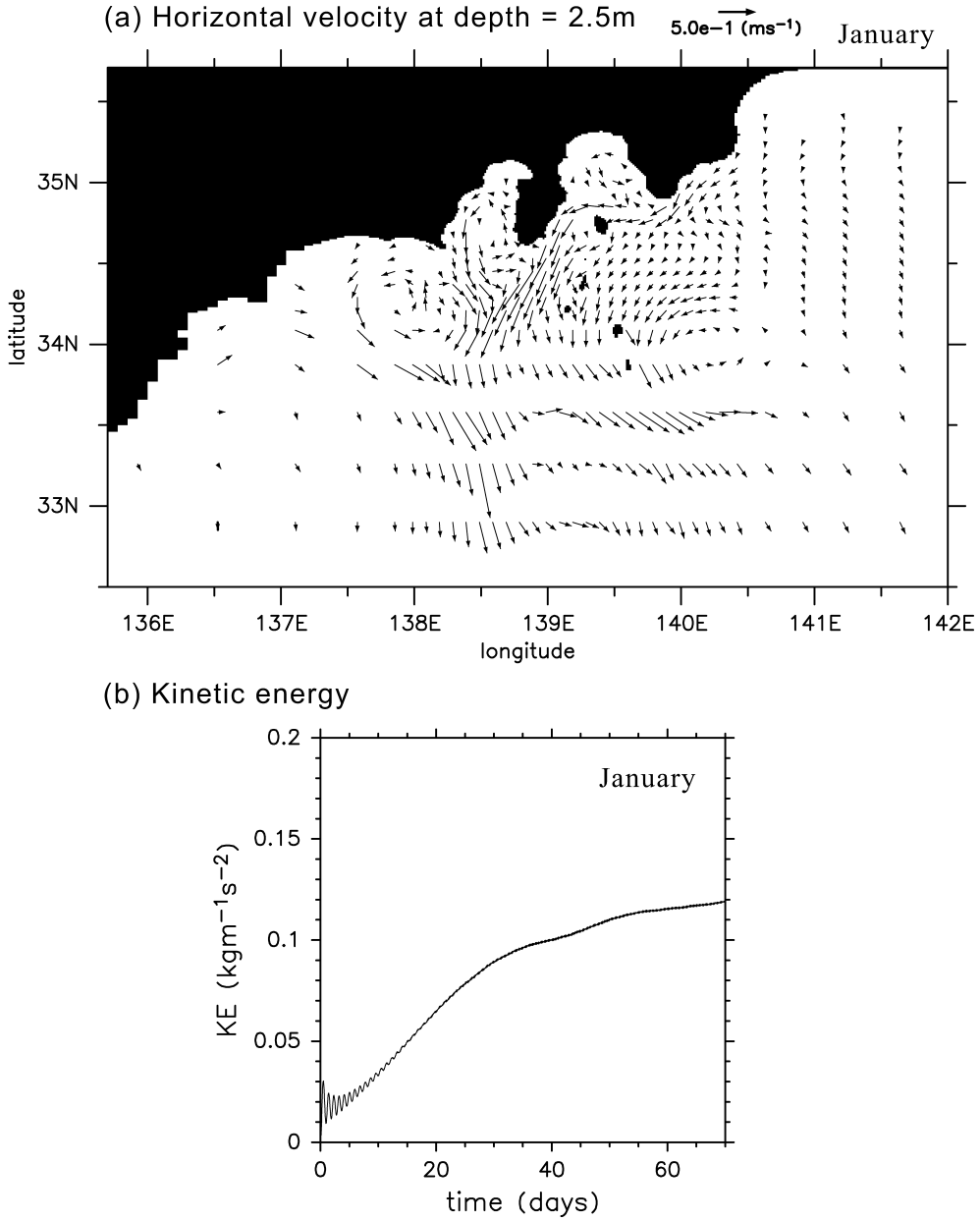

Fig. 5. (a) Horizontal velocity at vertical level 1 (depth 2.5 m) on day 60 in the case of January. (b) Time change of kinetic energy integrated over the model domain in the case of January.

any other case. The circulation reaches latitude 35.0°N, crossing the Senoumi Bank, whose location is indicated by an arrowin Figure 3b, and associated flow velocity is greater than 0.2 m s^{-1}. A similar counterclockwise circulation is generated across the bay mouth in April, although it is somewhat weak and does not cross the bank (Figure 6b). In addition, a weak small-scale clockwise circulation is generated to the north of the counterclockwise circulation in both cases. Furthermore, another weak small-scale counterclockwise circulation is generated in the most inner part of the bay in April.

In July and October, on the other hand, a clockwise circulation is generated just outside of the bay (Figures 6c and d). In addition, a counterclockwise circulation is generated within the bay in July, whereas a clockwise circulation in October. The counterclockwise circulation in July is located in the middle part of the bay, whereas the clockwise circulation in October is located in the inner part of the bay.

The circulations mentioned above are geostrophic, as the surface water tends to flow along isopleths of the sea surface height shown in Figure 7, which is calculated diagnostically from the prognostic variables (Pacanowski, 1996). In particular, the circulations that are generated across or just outside of the bay mouth are stronger than any other in the bay, and they rotate in the same direction as the wind stress forcing (Figure 1). The circulation scale seems to be strongly influenced by the bay's size and the bank.

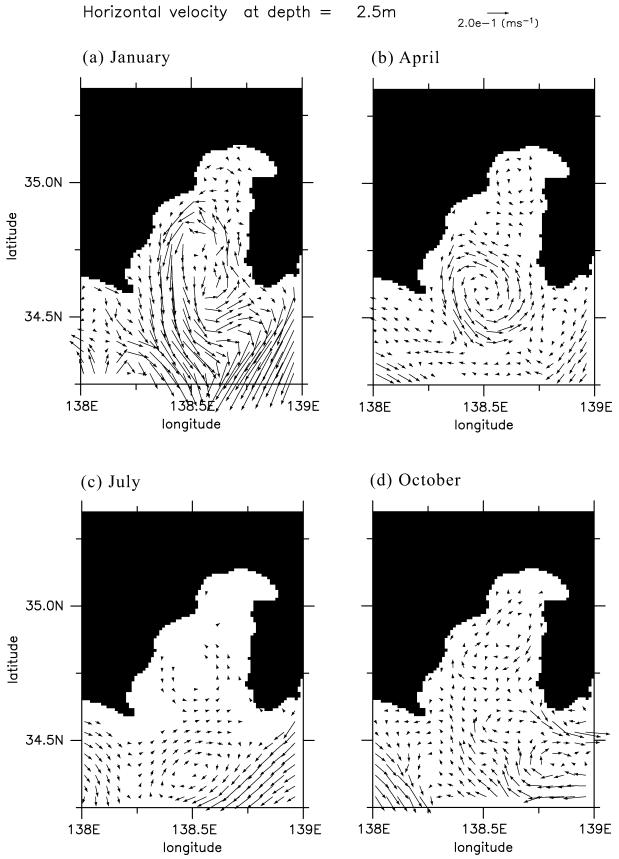

Fig. 6. Horizontal velocity at vertical level 1 (depth 2.5 m) in Suruga Bay on day 60. The figures cover only the region enclosed with a solid line in Figure 3: (a) January, (b) April, (c) July, and (d) October.

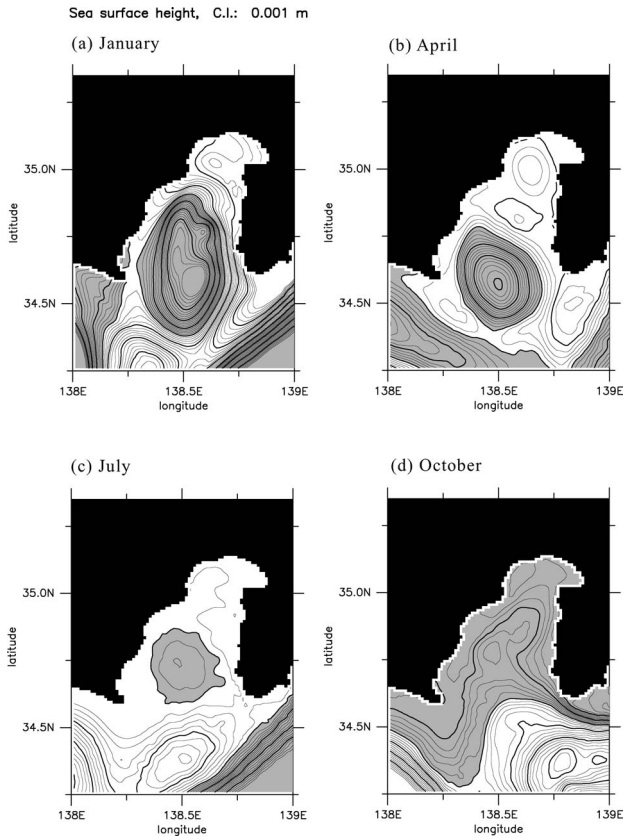

Fig. 7. Horizontal distributions of diagnostic sea surface height on day 60. Spatial mean is removed from the data, and the shaded regions indicate negative ones: (a) January, (b) April, (c) July, and (d) October.

Therefore, combined effects of the Earth' rotation (geostrophy), the vorticity of the wind stress (vertical component), and the topography of land and ocean bottom play essential roles in producing the circulations in and around the bay.

Inaba (1988) has suggested that two or three long-term circulations exist in Suruga Bay, whose rotation directions change depending on location of the Kuroshio current. That is, according to his schematic diagram, three circulations with counterclockwise, clockwise and another counterclockwise rotations tend to appear in the mouth, middle and inner parts of the bay, respectively, when the Kuroshio current flows north of the Zenisu Ridge. On the other hand, two circulations with clockwise and counterclockwise rotations tend to appear at the mouth and middle to inner parts of the bay, respectively, when the Kuroshio current flows south of the Zenisu Ridge. However, the present experiment shows that similar circulation patterns are produced without the effect of the Kuroshio current, suggesting that their change can be triggered only by the seasonal variation of the wind field in the real ocean.

To examine how deep the surface forcing penetrates into the ocean interior, Figures 8 and 9 show distributions of horizontal velocity at 368.5 m depth (in the intermdeiate layer below the thermocline, vertical level 11) and at 980.0 m depth (in the lowest layer of the model), respectively. The Senoumi Bank forms the boundary between circulations at 358.5 m depth in all cases, acting like a barrier to intrusion of open ocean waters (Figure 8). At this depth, the circulation around the bay mouth tends to have the same sign of vorticity as the surface circulation. However, the associated flow velocity is about one order of magnitude smaller than the surface velocity. (Note that the vector scale is an order of magnitude smaller in Figure 8 than in Figure 6.) Moreover, flows that are induced in the inner part of bay appear not to be closely related to the surface circulations, but to be strongly influenced by the bottom topography. Furthermore, there is almost no flow at 980.0 m depth (Figure 9). As a result, distributions of the stream function ψ (Figure 10), which is defined by $\partial\psi/\partial y = -\int_{-h}^{0} u\,dz$ with the water depth h, show similar patterns to those of the sea surface height (Figure 7). In other words, since the flows are very weak in the deep layers, the depth-integrated volume transport is mainly determined by the surface circulations.

Figure 11 shows distributions of vertical velocity in the sea surface layer, to which a five-grid running mean is applied in both longitudinal and latitudinal directions. In Janu-

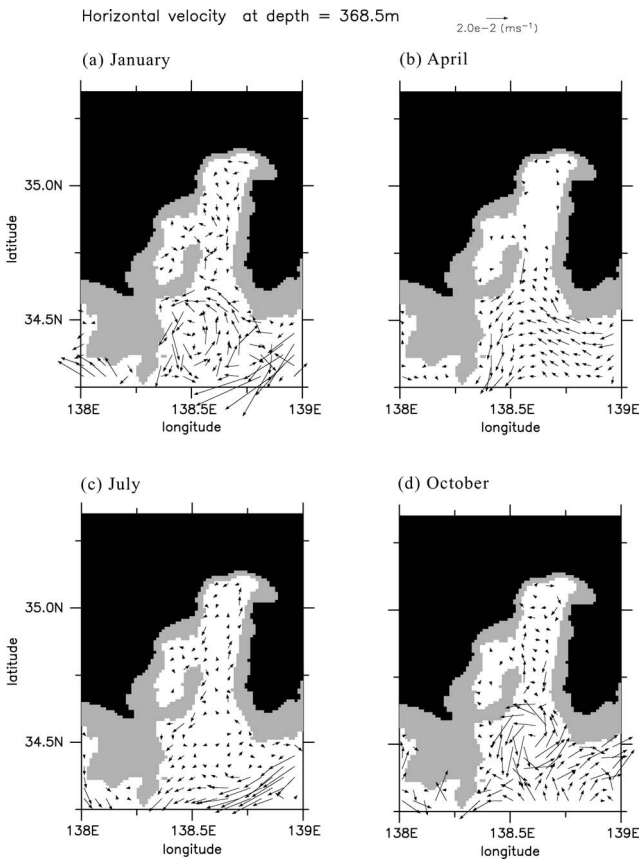

Fig. 8. Same as Figure 6, but for vertical level 11 (depth 368.5 m).

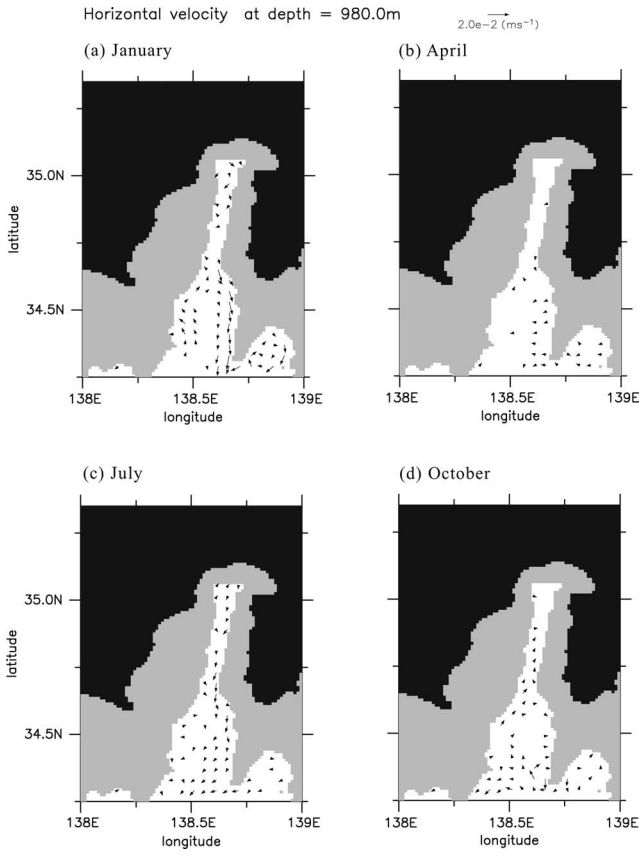

Fig. 9. Same as Figure 6, but for vertical level 14 (depth 980.0 m).

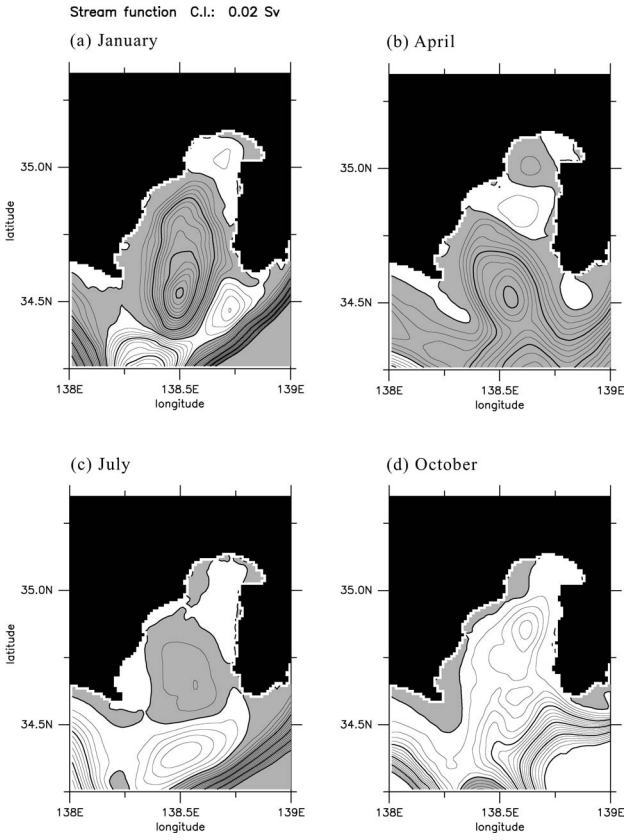

Fig. 10. Stream function (i.e., along which vertically-integrated mass transport flows) on day 60. Contour interval is 0.02 *Sverdrup* ($=0.02\times10^6\,m^3\,s^{-1}$). The shaded regions indicate negative values: (a) January, (b) April, (c) July, and (d) October.

ary, April and July, downward flows (indicated by shaded regions in Figure 11) exist mainly in the eastern part of the bay, indicating convergence of the surface waters in those regions. Moreover, Figure 12 shows distributions of the regions where horizontal velocity is smaller than the value of 2.0×10^{-2} $m\,s^{-1}$, and at the same time the vertical velocity is negative value in Figure 11. That is, this figure shows quasi-stagnant and convergent regions, suggesting that floating materials (flotages) may be accumulated there in the real ocean. Indeed, floating seagrass has been observed more in the eastern part of the bay than in the western part in May (Michida et al., 2006). Moreover, according to fishermen based in Heda Port (private communication; location of the port is indicated by an arrow in Figure 12a), a large amount of piled-up seagrass has been observed on the ocean floor at some areas off the port. Thus, there is a possibility that the wind-driven circulations may make an important contribution to the seagrass transport from in and around the bay to the eastern part of the ay, where the seagrass may have sunk to the ocean bottom.

Conclusion

We have investigated influence of the seasonal variation

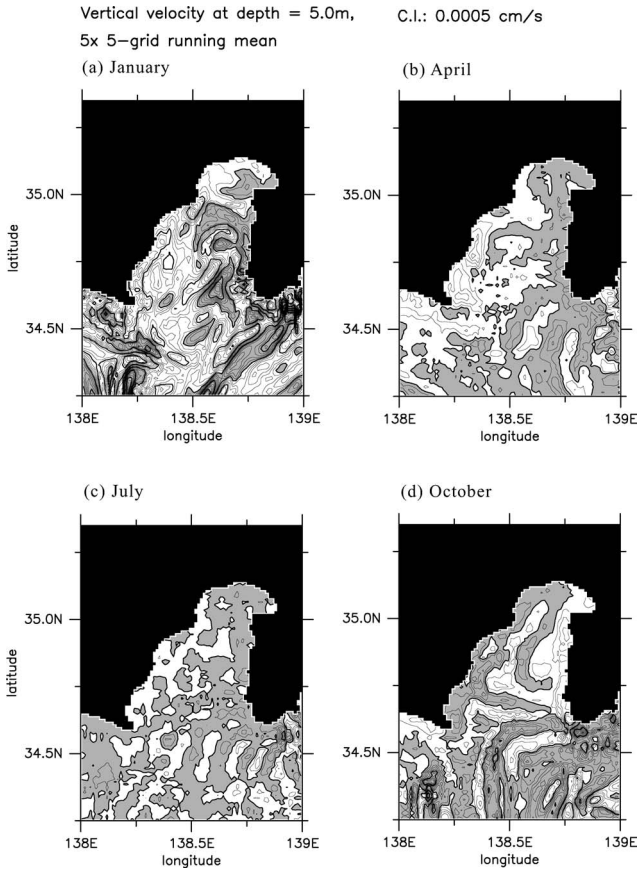

Fig. 11. Horizontal distributions of vertical velocity near sea surface (at depth 5 m) on day 60. A five-grid running mean is applied to the data in both longitudinal and latitudinal directions. The shaded regions indicate negative values, i.e., downward velocity: (a) January, (b) April, (c) July, and (d) October.

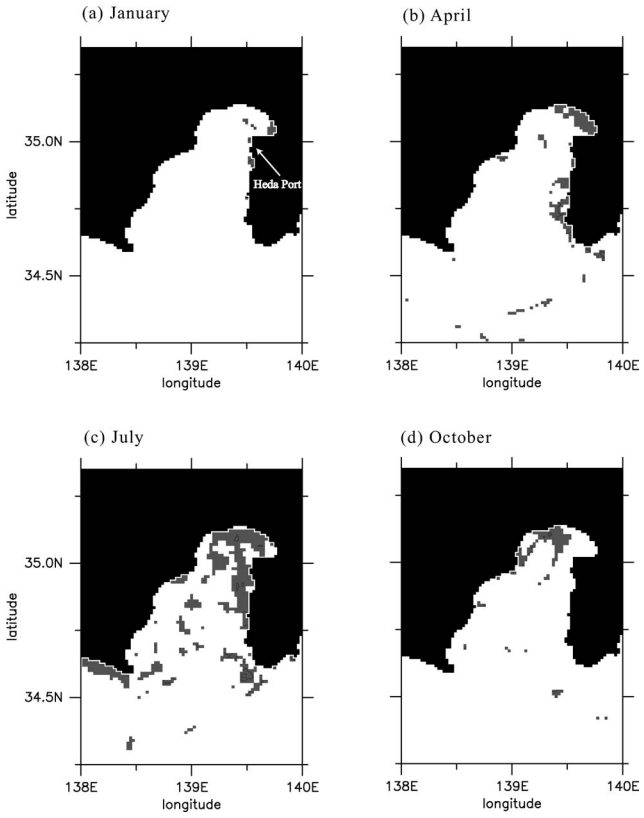

Fig. 12. Horizontal distributions of quasi-stagnant and convergent regions where horizontal velocity is smaller than the value of $2.0\times10^{-2}\,\mathrm{m\,s^{-1}}$, and at the same time the vertical velocity is negative value in Figure 11: (a) January, (b) April, (c) July, and (d) October.

in the wind field on the water circulations in Suruga Bay by using a wind data set based on objective analysis, and a numerical ocean model with realistic topography. Our focus is on wind-driven circulations, considering model's initial conditions in which fluid is at rest and potential temperature and salinity fields are horizontally uniform, but whose vertical profile is realistic. We have performed four experimental cases (January, April, July and October), in which the circulations are driven only by the monthly mean wind stress. In each experimental case, the wind stress is constant in time. The following results have been obtained:

Counterclockwise (positive) vorticity is supplied around the bay mouth from the atmosphere into the ocean in January (winter) and April (spring), whereas clockwise (negative) vorticity is supplied in July (summer) and October (autumn). This is because, in January and October, the wind stress forcing is reduced inside of the bay, whereas it is strong outside of the bay. There exist strong westerly and easterly winds outside of the bay in January and October, respectively. On the other hand, there are only weak winds in April and July. However, the weak westerly winds rotate counterclockwise in the bay in April, whereas clockwise in July.

Corresponding to these changes in the wind field, a counterclockwise circulation is generated at the sea surface across the bay mouth in January and April. The circulation is especially strong in January, crossing the Senoumi Bank, and associated flow velocity is greater than $0.2\,\mathrm{m\,s^{-1}}$. In addition, a weak small-scale clockwise circulation is generated to the north of the counterclockwise circulation in both months. Furthermore, another weak small-scale counterclockwise circulation is generated in the most inner part of the bay in April.

In July and October, on the other hand, a clockwise circulation is generated just outside of the bay. In addition, a counterclockwise circulation is generated within the bay in July, whereas a clockwise circulation in October. The counterclockwise circulation in July is located in the middle part of the bay, whereas the clockwise circulation in October is located in the inner part of the bay.

The above circulations, which are quasi-geostrophic and strongly influenced by the topography of land and ocean bottom, are generated without effect of the Kuroshio current, although the circulation patterns are similar to those suggested by Inaba (1988).

Flows are weak in the intermediate and deep layers, es-

pecially in the inner part of the bay (to the north of the Senoumi Bank). The Senoumi Bank forms the boundary between circulations in the intermediate layer, acting like a barrier to intrusion of open ocean waters. The depth-integrated volume transport is mainly determined by the surface circulations.

Quasi-stagnant and convergent regions exist in the eastern part of the bay during the whole year, except for autumn. Thus, there is a possibility that the wind-driven circulations may have transported the floating materials, such as seagrass, from in and around the bay to the eastern part of the bay, where a large amount of piled-up seagrass has been observed on the ocean bottom.

Since the present experiment has been performed with idealized formulation, there remain important problems for application to the real ocean. As mentioned in the introduction, the actual circulations in Suruga Bay will be driven also by various factors including effects of the Kuroshio current, river discharge and tides, other than the wind effect. In particular, the effects of the Kuroshio current may be very important to the long-term circulations. However, the simulated flow field may not be necessarily realistic off the Suruga and Sagami Bays (Figure 5a), where the Kuroshio and/or Kuroshio branch currents usually exist in the real ocean. Besides, lack of long-term observation records makes it difficult to ensure that the circulations with seasonal variation are generated by the winds in the real ocean. In future, we need to compare the present results with observational data not only from an Eulerian viewpoint, but also from a Lagrangian one using information about floating materials such as seagrass. Nevertheless, the present study gives important insight into the generation mechanism of the circulations in Suruga Bay, since the wind effect on the long-term circulations hardly been investigated to date.

Acknowledgements

The figures were produced by GFD-DENNOU Library. This research was partially supported by Ocean Research Institute, Tokyo University, Grant-in-Aid for Cooperation Studies, 2004–2005.

References

Igeta, Y., Kitade, Y. and Matsuyama, M. 2003. Numerical experiments on the Kyucho current in Sagami Bay associated with coastal-trapped waves caused by Typhoon 8818. Oceanogr. in Japan (Umi no Kenkyu) 12: 603–616 (in Japanese with English abstract).

Inaba, H. 1981. Circulation pattern and current variations with respect to tidal frequency in the sea near the head of Suruga Bay. J. Oceanogr. Soc. Japan, 37: 149–159.

Inaba, H. 1982. Relationship between the oceanographic conditions of Suruga Bay and locations of the Kuroshio path. Bull. Coastal Oceanogr. (Engan Kaiyo Kenkyu Noto). 19: 94–102 (in Japanese).

Inaba, H. 1984. Current variation in the sea near the mouth of Suruga Bay. J. Oceanogr. Soc. Japan 40: 193–98.

Inaba, H. 1988. Oceanographic environment of Suruga Bay—Fluctuation of oceanic and tidal current and temperature—. Bull. Japan. Soc. Fisheries Oceanogr. (Suisan Kaiyo Kenkyu). 52: 236–243 (in Japanese).

Katsumata, T. 2004. Intrusion process of oceanic water to Suruga Bay. PhD thesis. Tokai Univ. (in Japanese).

Kutsuwada, K. 1998. Impact of wind/wind-stress field in the North Pacific constructed by ADEOS/NSCAT data. J. Oceanogr. 54: 443–456.

Large, W. G. and Pond, S. 1981. Openocean momentum flux measurements inmoderate to strong winds. J. Phys. Oceanogr. 11: 324–336.

Matsuyama, M., Ohta, S., Hibiya, T. and Yamada, H. 1993. Strong tidal currents observed near the bottom in the Suruga Trough, Central Japan. J. Oceanogr. 49: 683–696.

Michida, Y., Ishigami, K., Komatsu, T. and Asano, K. 2006. Divergence field observed with surface drifters in Suruga Bay. Monthly Kaiyo. 38, No. 8: 547–552 (in Japanese).

Nakamura, Y. and Sawada, T. 1971. A characteristic of oceanographic structures in autumn 1969. Cruise summary report on Suruga Bay (Suruga-wan Kaiyo Chosa Hokoku) I. Shizuoka Pref. Fish. Exp. Stat, Shizuoka (In Japanese).

Officer, C. B. 1976. Physical Oceanography of Estuaries. John Wiley & Sons, New York.

Pacanowski, R. C. 1996. MOM 2.2β, documentation, user's guide and reference manual. GFDL Ocean Technical Report 3.2. Geophysical Fluid Dynamics Laboratory, Princeton.

Rosati, A. and Miyakoda, K. 1988. A general circulation model for upper ocean simulation. J. Phys. Oceanogr. 18: 1601–1626.

Smagorinsky, J. 1963. General circulation experiments with the primitive equations: I. The basic experiment. Month. Weather Rev. 91: 99–164.

Stevens, D.P. 1990. On open boundary conditions for three dimensional primitive equation ocean circulation models. Geophys. Astrophys. Fl. Dyn. 51: 103–133.

Takeuchi, K. and Hibiya, T. 1997. Numerical simulation of baroclinic tidal currents in Suruga Bay and Uchiura Bay using a high resolution level model. J. Oceanogr. 53: 539–552.

Unoki, S. and Okami, N. 1985. Coastal currents in Suruga Bay and Enshu-nada deduced from LANDSAT MSS images. Bull. Japan. Soc. Fisheries Oceanogr. (Suisan Kaiyo Kenkyu). 47–48: 1–10 (in Japanese).